ADVANCED OPTICAL MATERIALS
www.advopticalmat.de

Materials Views
www.MaterialsViews.com

Unraveling Bright Molecule-Like State and Dark Intrinsic State in Green-Fluorescence Graphene Quantum Dots via Ultrafast Spectroscopy

Lei Wang, Shou-Jun Zhu, Hai-Yu Wang, Ya-Feng Wang, Ya-Wei Hao, Jun-Hu Zhang, Qi-Dai Chen, Yong-Lai Zhang, Wei Han, Bai Yang,* and Hong-Bo Sun**

Graphene quantum dots (GQDs) have recently emerged as a promising type of low-toxicity, high-biocompatibility, and chemically inert fluorescence probe with a high resistance to photobleaching. They are a prospective substitution for organic materials in light-emitting devices (LED), enabling the predicted concept of much brighter and more robust carbon LED (CLED). However, the mechanism of GQD emission remains an open problem despite extensive studies conducted so far, which is becoming the greatest obstacle in the route of technical improvement of GQD quantum efficiency. This problem is solved by the combined usage of femtosecond transient absorption spectroscopy and femtosecond time-resolved fluorescence dynamics measured by a fluorescence upconversion technique, as well as a nanosecond time-correlated single-photon counting technique. A fluorescence emission-associated dark intrinsic state due to the quantum confinement of in-plane functional groups is found in green-fluorescence graphene quantum dots by the ultrafast dynamics study, and the two characteristic fluorescence peaks that appear in all samples are attributed to independent molecule-like states. This finding establishes the correlation between the quantum confinement effect and molecule-like emission in the unique green-fluorescence graphene quantum dots, and may lead to innovative technologies of GQD fluorescence enhancement, as well as its broad industrial application.

1. Introduction

Similar to other popular carbon nanomaterials such as graphene,[1] graphene oxide (GO),[2] and quasi-spherical carbon nanodot (C-dot),[3] recently emerging graphene quantum dots (GQDs) have been attracting more and more research attention due to their superiority in chemical inertness, resistance to photobleaching, low toxicity, excellent biocompatibility, low cost and abundance in nature.[4] As disc-like nanocarbons with diameter from several nanometers to tens of nanometers, consisting of one or a few graphite layers, GQDs generally possess abundant functional groups decorated at surface, which impart GQDs with excellent solubility and suitability for subsequent functionalization with other organic or inorganic species, thus greatly widening their applications. With proper surface decoration, GQDs display fascinating photoluminescence (PL) properties, i.e., excitation wavelength-dependent emission, pH-sensitive luminescence intensity, and up-conversion PL, which are also observed in C-dots.[5,6] These features bring fluorescent GQDs large potential in many application areas such as biosensor, bioimaging, photovoltaic conversion and photocatalysis.[7,8] Even the concept of carbon light-emitting diodes (CLEDs) could be enabled if GQDs were adopted as an alternative to organic active materials. The CLED may exhibit much higher carrier transport mobility, longer lifetime and better robustness compared with the currently available OLEDs. Despite all these unique performance, there is a long way to go before the above dreams come true because of a lot of technical problems that still need solving, particularly the GQD quantum efficiency improvement and the emitting wavelength design. However, the origin of the fascinating photoluminescence emission behaviors is still a matter of current debate, as becomes the major obstacle to reach the above ends. Without understanding of fluorescent mechanism, it would not be possible to effectively synthesize GQD samples with desired brightness and working wavelength, and design appropriate photonic and electronic structures to fulfilled required device functions.

L. Wang, Prof. H.-Y. Wang, Y.-W. Hao, Dr. Q.-D. Chen, Y.-L. Zhang, Prof. H.-B. Sun
State Key Laboratory on Integrated Optoelectronics
College of Electronic Science and Engineering
Jilin University
2699 Qianjin Street, Changchun, 130012, China
E-mail: haiyu_wang@jlu.edu.cn; hbsun@jlu.edu.cn
Y.-F. Wang, Prof. W. Han, Prof. H.-B. Sun
College of Physics
Jilin University
2699, Qianjin Street, Changchun, 130023, China
S.-J. Zhu, Dr. J.-H. Zhang, Prof. B. Yang
State Key Laboratory of Supramolecular Structure and Materials
College of Chemistry
Jilin University
2699, Qianjin Street, Changchun, 130023, China
E-mail: byangchem@jlu.edu.cn

DOI: 10.1002/adom.201200020

It is not surprising that various spectroscopic technologies has been considered and utilized as the most efficient means to reveal the GQD emission scenario. In steady-state spectroscopy, GQDs typically present strong absorption in UV region with a tail extending into visible range. But the PL is varied in a large range from deep ultraviolet to green even yellow, when GQDs are prepared by different synthesis method. In combination with nanosecond time-resolved PL dynamics, several presumed PL mechanisms are proposed such as edge effect or quantum size effect.[9,10] These mechanisms could explain themselves, but sometimes it seems to be inconsistent with each other. For example, a size dependent PL was observed in one kind of GQDs from acidic treatment of carbon fibers.[11] However, in another kind of GQDs prepared by microwave-assisted hydrothermal method, the emission wavelength is independent of the size of the GQDs, which could be related to the self-passivated layer of GQDs.[12] This shows that some crucial details are hidden in the steady-state characterizations. It also implies that these relevant events may happen very fast which are far beyond instrument resolution of nanosecond time-resolved equipment. In a kind of colloidal GQDs synthesized by a solution chemistry method on the basis of bottom-up approach, Li and co-workers reported slow hot carrier relaxation investigated via femtosecond monochromatic transient absorption spectroscopy, although the GQDs in their study have a significant probability of relaxing into triplet states that is absent in other GQDs synthesized by different method.[13,14] Since only femtosecond pump-probe method was used in their work, it could not obtain more information about the PL. But it already indicates that these interesting excited-state processes, i.e., carrier relaxation, electron transfer and recombination which usually occur within hundreds of picoseconds, are the key to reveal the PL origin. Therefore, a requirement for detailed ultrafast dynamics study on GQDs by femtosecond time-resolved spectroscopy becomes indispensable, which could make important contributions in this nascent quantum dots as it did in other fields.[15–17]

Here, we choose green-fluorescence GQDs with high photoluminescence quantum yield (QY ~ 12%) and oxidation degree (~41%, including carboxylic, hydroxyl, epoxy, carbonyl groups, and so on), which are synthesized from a two-step method combining 'top-down' cutting GO and separation routes.[18] A schematic representation of this kind of GQDs is presented in **Figure 1**a, in which some characteristic functional groups decorate the basal plane and lateral edge. According to the previously expected manipulation that simultaneously modifying the band structure of graphene by reduced size and surface chemical functionalization, GQDs have the capability of opening the band gap of bulk graphene and leading to a strongly tunable PL which is dependent on size or oxidation degree.[19–24] In theory, besides the factor of size, these characteristic functional groups in plane, such as hydroxyl and epoxy groups which play the role of potential well, also could provide quantum confinement, and lead to discrete quantum states. After redistribution of these quantum states, the resulted GQDs could open a band gap. In practice, the role of quantum confinement effect in GQDs still needs to be tested, owing to the possible synergy or competition with size and edge effect. Figures 1b and c show that the average diameters of GQDs are 3–5 nm and the average height is 0.95 nm, according to TEM and AFM image, respectively. We wonder what would happen in such a small particle when it is excited by absorbing high energy photons. Since the steady-state absorption and emission properties of green-fluorescence GQDs are well representative in fluorescent carbon nanomaterials,[25–27] a detailed ultrafast dynamics study on origin of their PL will be of great significance. Thus, a combination of femtosecond broadband transient absorption (TA) spectroscopy and femtosecond time-resolved fluorescence dynamics measured by fluorescence upconversion technique, as well as nanosecond time-correlated single-photon

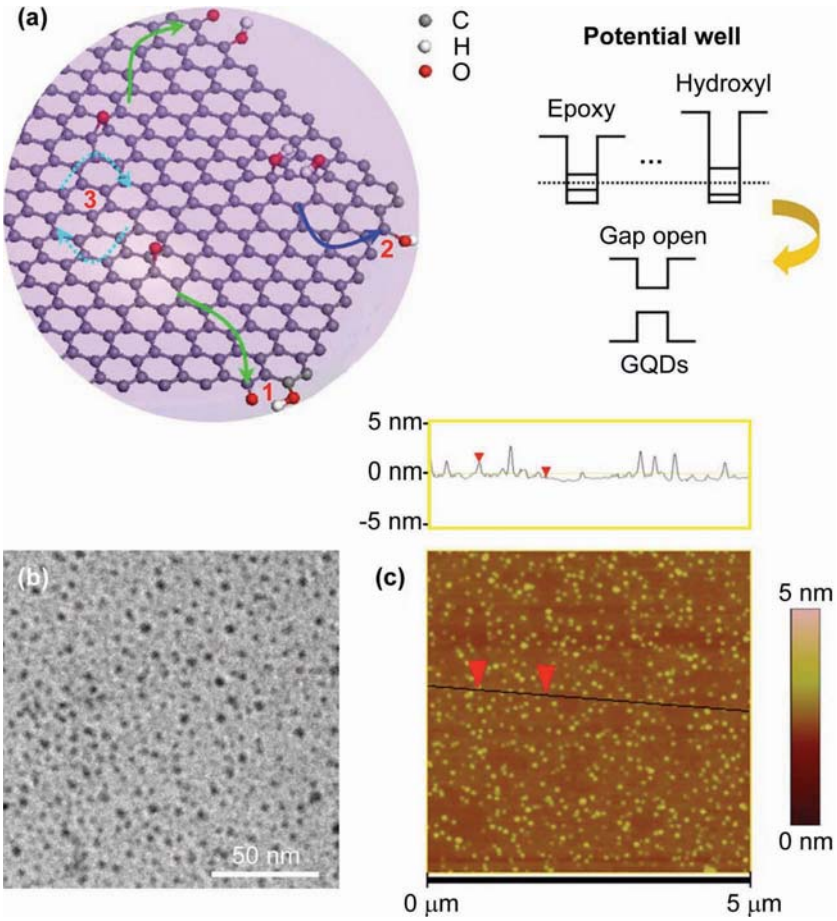

Figure 1. (a) Left: schematic representation of green fluorescence GQDs containing characteristic functional groups in plane and at edge. The number 1–3 represent the three kinds of emission states revealed by ultrafast spectroscopy (see detailed discussion below). Right: the effect of functional groups in plane: open the band gap and stabilize the ground state relative to the excited state. (b) TEM and (c) AFM image of green fluorescence GQDs. The average diameters of GQDs are 3–5 nm, and the average height is 0.95 nm.

counting (TCSPC) technique is performed. The observation of spectrally resolved ultrafast dynamics enables us for the first time to expose the ultrafast excited state process, identify the possible recombination approach, and finally unravel the mechanism of photoluminescence in GQDs. Our research reveals that three kinds of emission states (assigned 1–3 in Figure 1a) could be found in the green-fluorescence GQDs, and hence, a physical picture on mechanism of PL is beginning to gradually come out.

2. Results and Discussion

2.1. Steady-State Absorption and Photoluminescence

Typically, there are two bands in the steady-state absorption spectrum (**Figure 2**a). One is subtle and located at around 320 nm, which is assigned according to previously reports (State 1),[18,20,21] and the other is located at around 400 nm (State 2) with a tail. Due to the overlapping with the absorption of carbon backbones, the peaks seem weak and subtle. However, if we subtract the background absorption, i.e., the absorption of grapheme oxide (GO) as we shown in Figure S1, these peaks immediately become much easier for identification. The two absorption bands are more evident in photoluminescence excitation (PLE) spectra (Figure 2b), which represent the absorption lines of corresponding PL. The PLE spectrum (PLE 430 nm and PLE 530 nm) reflects that the emission at 430 nm and 530 nm is solely resulted from States 1 and 2, respectively.

2.2. Time-Resolved Photoluminescence Dynamics

Seemingly, the green fluorescence should arise from a state like the band edge state or trap state if we associate the GQDs with semiconductor quantum dots. This intuitive idea is very attractive but still lack of evidence. Whether are there some new findings according to our ultrafast dynamics study? To answer this question, we first examine the nanosecond fluorescence lifetime of different wavelength by TCSPC technique. Since at this moment our preferential concern is the origin of green fluorescence, excitation wavelength is adopted at 405 nm for only exciting State 2. Lifetime components extracted from TCSPC data are presented in **Figure 3**a. This aim is to find whether

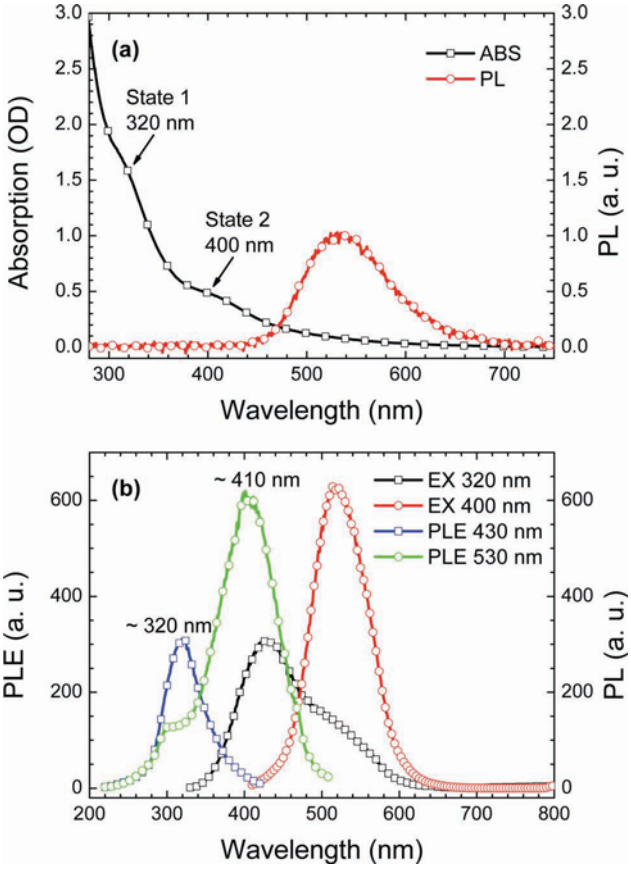

Figure 2. (a) Steady-state absorption (black) and emission (red) spectra of green fluorescence GQDs in water at 400 nm excited. (b) Emission (black and red) and corresponding photoluminescence excitation (blue and green) spectra.

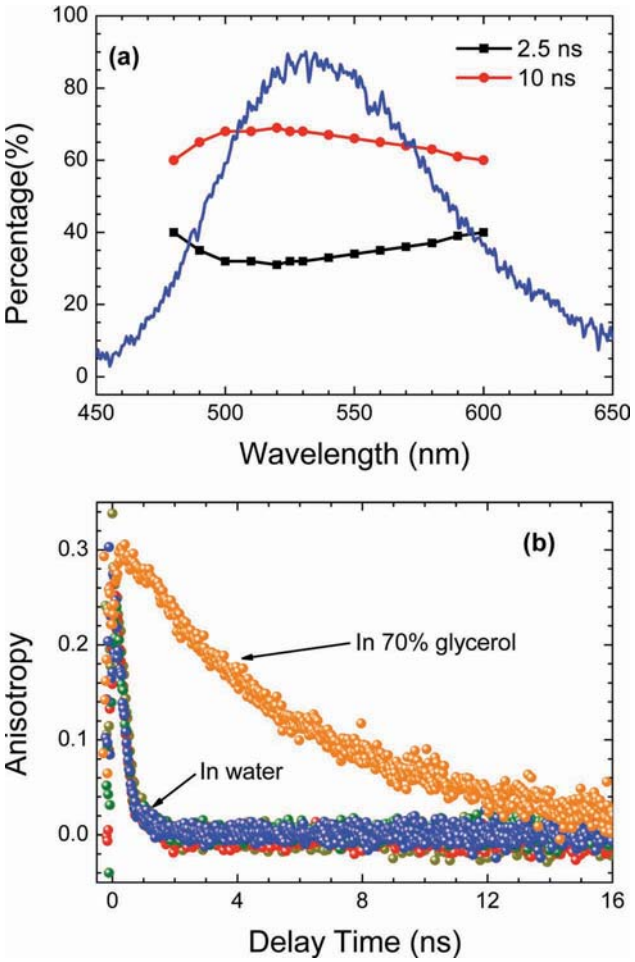

Figure 3. (a) Lifetime components extracted from TCSPC data of GQDs at different probe wavelength excited at 405 nm. The blue line is the corresponding steady-state PL spectrum. (b) Anisotropy study of GQDs in water and 70% glycerol aqueous solution.

there is a series process of electron trapping. If the electron trapping occurs, the red side of PL will present longer lifetime than that of PL peak, while the lifetime of blue side will shorter. However, the resulted average lifetime around PL peak is 7.7 ns and only contains two lifetime components, which is 2.5 ns (~30%) and 10 ns (~70%). Although the ratio of two lifetime components at the blue side and red side of PL presents a few changes, the average lifetime almost keeps the same, 7 ns, which is slightly shorter than that around PL peak. It implies this green fluorescence state is too simple due to surface trap states as in semiconductor quantum dots, like CdS QDs.[28,29]

In addition, the fluorescence anisotropy of GQDs in the whole emission range rightly has a nearly same initial value 0.3, and same decay time (Figure 3b). Since the theoretical maximum of anisotropy is 0.4, and only in some special case, i.e., existing two excited states with perpendicular transition dipoles, this maximum in the whole emission range will decrease to 0.3, it implies that two excited states could exist in GQDs, and the transition dipole of another excited state could be perpendicular to State 2. This excited picture is confirmed in the later femtosecond time-resolved experiments. Moreover, this identical aging of anisotropy indicates that there is no step-trapping or energy migration process in the GQDs. So, the fluorescence anisotropy decay is simply due to the rotational diffusion motion of the GQDs as a whole. This is confirmed by the much slow anisotropy decay in 70% glycerol aqueous solution. The glycerol increases the viscosity of solution, and then slows down the rotational diffusion of samples. By one-exponential fitting, we obtain a rotational diffusion time, τ_{rot} = 300 ps and 6 ns in water and 70% glycerol aqueous solution, respectively, which is in agreement with the theoretical expectation (see detail in the supporting information, Anisotropy analysis). The resulted rotational diameter is about 1 nm, which is consistent with the average height (0.95 nm) of GQDs very well. This indicates GQDs have a pure rotation process in slip case.

To scrutinize the origin of green fluorescence, subpicosecond time resolved fluorescence dynamics measured by fluorescence upconversion technique were performed at 400 nm excitation (also only State 2 is excited) to observe the faster process. As shown **Figure 4**, the femtosecond to picosecond photoluminescence decay kinetics shows that all of these wavelengths ranging from the blue side to red side of PL have a same long lifetime (normalized to the long delay time), which are correspond to TCSPC results. All the transients have an instantaneous rise. For the red side of the green fluorescence (wavelength beyond 530 nm), there is no fast decay. But for the blue side, it is a different case. The shorter wavelength has a larger fast decay component with time constant range from 200 fs to 1.6 ps. Does this imply there are two emission states? Temporarily, we name the two states are intrinsic state (corresponding to the fast lifetime) and surface state (corresponding to the long fluorescence lifetime).

2.3. Femtosecond Transient Absorption Spectroscopy

As a necessary complement, broadband (350–750 nm) TA experiments are also performed at 400 nm excitation. Usually, there are three kinds of spectral features in TA spectrum.

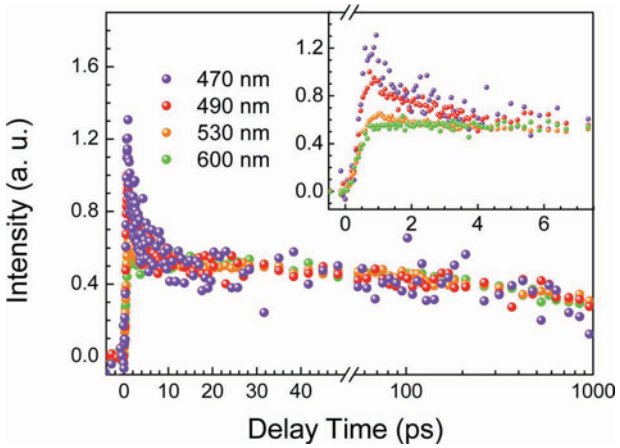

Figure 4. Femtosecond time-resolved PL data of GQDs at different probe wavelength excited at 400 nm. Inset is the traces in the first several picoseconds.

After the pump light excitation, due to the Pauli exclusion principle, the filling of quantized electronic states will lead to the bleaching of the corresponding optical transitions from ground state to excited state, which is named ground state bleaching (GSB). On the other hand, the photoexcited electrons in the excited states could further absorb probe light to higher levels or return to ground state by stimulated radiation due to the disturbance of probe light, which is so-called excited-state absorption (ESA) and stimulated emission (SE), respectively. Among the features, only excited-state absorption is positive signals, the other is negative signals. All of these features reflect the information about the change of photogenerated carrier populations in corresponding energy levels. From **Figure 5**a, one can clearly observe a positive excited-state absorption (ESA 1) signal at 475 nm. In the red side of ESA 1, a negative signal appears after the initial several picoseconds, which should be corresponding to simulated emission of green fluorescence according to steady-state PL spectrum. In the far blue side of ESA 1, there is another subtle signal at around 400 nm. It is negative within the first 1 to 2 ps (Figure S2). This signal could be attributed to ground state bleaching (GSB), which is relative to State 2. This bleaching signal is more obvious in the double difference spectrum between different delay times as shown in Figure 5b, see below. Within the first 5 ps, the transient spectra show a largely change around 560 nm, where the simulated emission band becomes more pronounced. By subtracting the spectrum at 0.6 ps with that at 5 ps, we get the double different spectrum that give the transient spectral change during the first 5 ps (Figure 5b). The double difference is equal to a differential process. For a decay dynamics, the double difference spectrum indeed is a negative signal. It clearly shows that the disappearance of an absorption band (peak around 560 nm) is accompanied with the GSB (around 400 nm) recovering. We should mention that no picosecond formation process is observed in PL results, so this simply reflects the decay out of another excited state absorption (ESA 2). At long time scale, the TA spectra show only ESA 1 and green-SE bands, and decay synchronously. These transient behaviors reflect two points: one is that the long lifetime components of ESA 1 and SE signal are

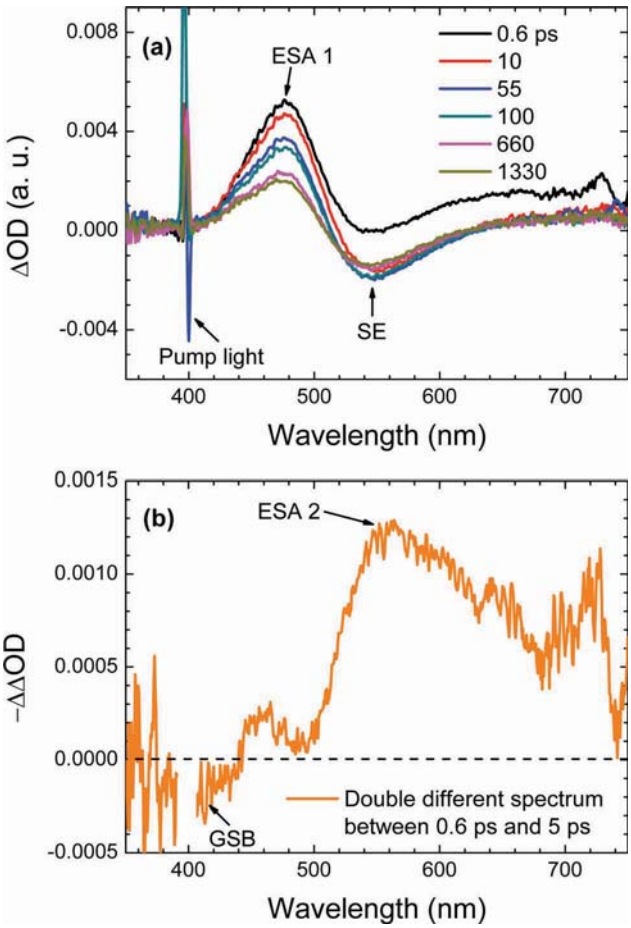

Figure 5. TA spectra (a) and double difference spectrum (b) of GQDs between different delay times. To rule out the influence of pump light, the spectral range from 390 nm to 405 nm corresponding to pump light was cut out in the double difference spectrum.

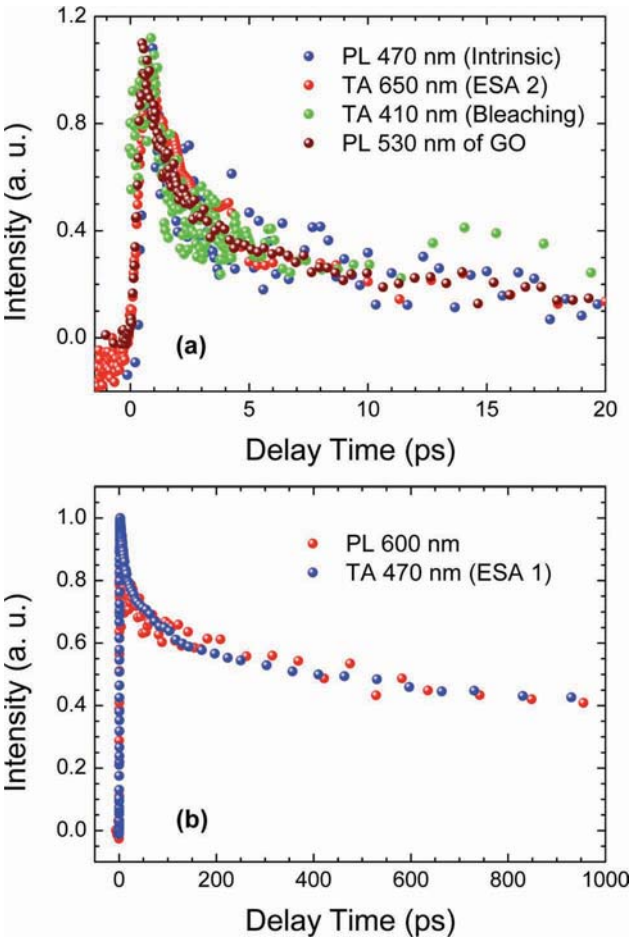

Figure 6. A comparison between TA and femtosecond time-resolved PL experiments. In panel (a), the long lifetime component of all the three wavelengths is subtracted; the origin data are presented in the supporting information, Figure S3.

identical and could be responsible for the green fluorescence; the other is that the ESA 2 signal is probably relevant to the GSB signal, and the both could be corresponding to an ultrafast recovery process of ground state. Pump-power dependent measurements are also carried out (not shown here). In the acceptable range, no pump intensity dependent dynamics are observed in the above mentioned characteristic signals. This intensity independent kinetics indicates that there is no carrier density dependent behavior in GQDs. It is totally different with semiconductor quantum dots, in which Auger like recombination is dominant. Up to now, two states (ESA 1 and ESA 2) are clearly identified in TA. The question is what the relation between these two states in TA with the two emission states found in femtosecond fluorescence dynamics.

2.4. Comparison and Analysis

To answer this question, the dynamics of TA transients are carefully compared with that of PL. As long as these characterization dynamics represent the same excited-state energy level, the comparison with each other is a powerful evidence for identifying the relaxation channel of excited state electron in the complex photophysics process. First, for the fast decay state, kinetics of three different characterization wavelengths, which are blue side of green fluorescence (470 nm in PL), GSB (410 nm in TA) and ESA 2 (650 nm in TA), respectively, are consistent very well as shown in **Figure 6**a. In order to avoid the influence of fluorescence signal, the wavelength of 650 nm in TA is adopted to represent ESA 2. This accounts for the origin of the blue side of the green fluorescence at around 470 nm. Namely, this part of PL arises from a ground state (intrinsic state), located at around 400 nm, with corresponding excited-state absorption ESA 2. Due to the fast decay, the photoluminescence quantum yield of this state is estimated to be very low, and it is almost no contribution to the steady-state fluorescence at 400 nm excitation. Second, the dynamics of long lifetime of ESA 1 (470 nm in TA) is indeed the same as that of red side of PL (600 nm in PL) shown in Figure 6b. This indicates that the strong green fluorescence originates from another state (surface state), which is corresponding to ESA 1. The surface state also has a ground state which is restored at around 410 nm (see the Supporting Information, Figure S4). Hence, the possibility that

the surface states arise from trap states is ruled out. Furthermore, considering the pH-dependent feature of the green fluorescence,[24] we conclude that this surface state corresponding to green fluorescence should be a molecule-like state.

The blue fluorescence (peak at 430 nm) is further taken into account when the band at around 320 nm is excited. Its average PL lifetime is about 4 ns according to TCSPC at 379 nm excitation (not shown here). The TA data at 320 nm excitation shows that only an excited state absorption with peak at around 540 nm occurs, and there is no wavelength-dependent dynamics (see the Supporting Information, Figure S5). These results suggest that it is also another molecule-like state. Thus, there are three emission states in the green-fluorescence GQDs. The last question is what relationship between the two molecule-like states. Since there is a superposition between the blue fluorescence excited at 320 nm and the absorption of surface state at around 410 nm, as well as the very close dipoles (GQD is only 3 nm), an efficient resonance energy transfer between the two states would be expected. However, the femtosecond time-resolved fluorescence data shows that the traces of green fluorescence under 320 nm and 400 nm excitation are overlapping (see the Supporting Information, Figure S6). Absent of energy transfer indicates the two dipoles are indeed perpendicular to each other.

The two bright molecule-like states could be relative to the functional groups, because these functional groups like carboxylic, hydroxyl and epoxy groups are necessary for the dissolution of GQDs and usually decorate the edge or in plane formed 'molecule states'.[30] In green fluorescence GQDs, we guess the synergy of carbonyl group and nearby hydroxyl group (assigned 1 in Figure 1a) maybe play an important role in the green fluorescence emission,[15] and the hydroxyl group alone decorated at the lateral edge or in plane (assigned 2 in Figure 1a) could account for the blue fluorescence, since the hydroxyl group decorated carbon nanomaterials usually emit blue fluorescence.[31] This implies that suitable surface chemical modification could change the emission states and hence exhibit tunable fluorescence.[32–34] Our study also first establishes the relationship between the PL of GQDs and surface molecule-like state. The corresponding molecule-like state will be readily reflected in the PLE spectrum, vice versa. Such as the case of blue-fluorescent GQDs,[9] the PLE peak at ~410 nm is totally disappeared and another new main PLE peak at 257 nm means there is another type of surface chemistry around these blue-fluorescent GQDs.

Thus, the dark intrinsic state at around 400 nm becomes more and more interesting. Therefore, we further examined the fluorescence dynamics of GO (see the Supporting Information, Figure S7), and surprisingly found it is overlapping with the kinetics of intrinsic state very well (Figure 6a). It implies that the intrinsic state in GQDs could be inherited from its precursor GO. This is reasonable that after cutting GO nanosheets to GQDs, the size, surface chemistry and edge of GO nanosheets are changed, but some physical properties in the basal plane still remain. In these regions of bare carbon backbone, although few functional groups decorate, the gap is still opened due to the quantum confinement of functional groups in plane. So, this evidence unambiguously indicates the intrinsic state (assigned 3 in Figure 1a) in GQDs is derived from the carbon backbone, in which a gap, around 3.1 eV, opens due to the quantum confinement.

Nowadays, according to the above presented analysis, we could conclude the quantum confinement in GQDs exhibits three unique features. First, the band gap state (intrinsic state) originated from quantum confinement of functional groups in plane is an optical dark state, and the fluorescence is mainly attributed to molecule-like states. Second, the molecule-like state is in dependent on the species and population of functional groups. The above two points explain the PL diversity of samples prepared by different synthesis methods, which seemingly shows a dependence of oxidation degree.[18,33] The last but not least, the synergic effect of quantum confinement and molecule-like emission could provide an additional PL property, enhancing the capability of resistance to photobleaching.[20] A band gap state with short fluorescence lifetime in GQDs means the particle could not only provide more electrons from ground state to the bright molecule-like state, but also have the capability of repeatedly utilizing the electron. This feature is obviously helpful for enhancing the photostability of GQDs.

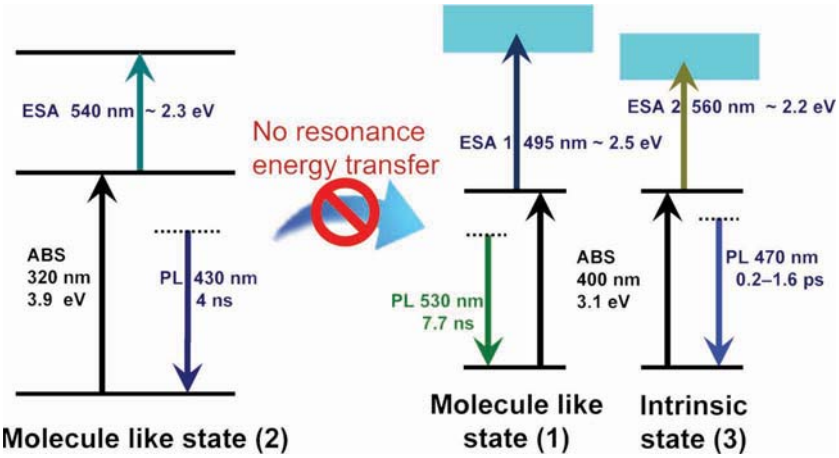

Figure 7. The photoluminescence picture in green-fluorescence GQDs. (ABS: absorption; PL: photoluminescence; ESA: excited-state absorption) Note that the peak position of ESA 1 is corrected (see detail in the Supporting Information, Figure S4).

3. Conclusion

In summary, a photoluminescence picture in green-fluorescence GQDs is clearly presented (**Figure 7**). An intrinsic band gap state accompanied with a molecule-like state (both at around 400 nm) is accounting for the strong green fluorescence with good photostability. The intrinsic state is attributed to quantum confinement, and its PL locates at around 470 nm with a dominant short lifetime and low photoluminescence quantum yield. Another irrelevant molecule-like state (around 320 nm) provides a blue fluorescence with peak at around 430 nm. The three kinds of emission states constitute the fascinating PL of green-fluorescence GQDs. It is worth noting that several

kinds of green-fluorescence GQDs or C-dots prepared by different synthesis method are reported.[18,20,21,27,35,36] This reflects that these phenomena attracted our attention in this green-fluorescence GQDs are common, and the proposed picture here is well representative. It will be of great benefit to understand the photophysics in GQDs and other carbon nanodots. Moreover, since the green fluorescence probably is relative to the surface functional group, our result suggests that proper surface chemical modification could be benefit to change the color of emission. Therefore, our proposed mechanism maybe could be extended to blue-luminescence samples after modest modification. At last, aiming for achieving higher fluorescence quantum yield or tunable emission wavelength, we need to collect more detailed information about the band gap state (intrinsic state) due to quantum confinement and the molecule-like state due to different molecule conformation. Hence, further transient experiments under different condition, such as changing pH, solvent and surface modification, are attractive and indeed underway.

4. Experimental Section

Time-Resolved Photoluminescence: Nanosecond fluorescence lifetime experiments were performed by the time-correlated single-photon counting (TCSPC) system under right-angle sample geometry. A 405 nm picosecond diode laser (Edinburgh Instruments EPL375, repetition rate 2 MHz) was used to excite the samples. The fluorescence was collected by a photomultiplier tube (Hamamatsu H5783p) connected to a TCSPC board (Becker&Hickel SPC-130). Time constant of the instrument response function (IRF) is about 300 ps.

Subpicosecond time resolved emission were measured by the femtosecond fluorescence upconversion method. A mode-locked Ti:sapphire laser/amplifier system (Solstice, Spectra-Physics) was used. The output of the amplifier of 1.5-mJ pulse energy, 100 fs pulse width, at 800 nm wavelength is split into two equal parts; the second harmonic (400 nm) of one beam was focused in the sample as excitation. The resulted fluorescence was collected and focused onto a 1 mm thick BBO crystal with a cutting angle of 35 degrees. The other part of the RGA output was sent into an optical delay line and served as the optical gate for the upconversion of the fluorescence. The generated sum frequency light was then collimated and focused into the entrance slit of a 300 mm monochromator. A UV-sensitive photomultiplier tube 1P28 (Hamamatsu) was used to detect the signal. The FWHM of instrument response function was about 400 fs.

Femtosecond Transient Absorption Setup: The TA setup consisted of 400 nm pump pulses doubled from 800 nm laser pulses (~100 fs duration, 250 Hz repetition rate) generated from a mode-locked Ti:sapphire laser/amplifier system (Solstice, Spectra-Physics) and broadband white-light probe pulses generated from 2-mm-thick water or 5-mm-thick CaF_2 substrate. The relative polarization of the pump and the probe beams was set to the magic angle. The TA data were collected by a fiber-coupled spectrometer connected to a computer. The group velocity dispersion of the transient spectra was compensated by a chirp program. All the measurements were preformed at room temperature. Pump-power dependent measurements are carried out. In the acceptable range, no pump intensity dependent dynamics are observed.

Supporting Information

Supporting Information is available from the Wiley Online Library or from the author.

Acknowledgements

The authors would like to acknowledge National Basic Research Program of China (973 Program, Grant No. 2011CB013005), the 863 project of China Grant No. 2013AA030902 and Natural Science Foundation, China (NSFC) under Grants No. 21273096, 20973081, 90923037, 60525412, 60677016, 20921003 and 10904049 for support.

Received: October 23, 2012
Revised: November 19, 2012
Published online: February 22, 2013

[1] A. K. Geim, K. S. Novoselov, *Nat. Mater.* **2007**, *6*, 183.
[2] Y. L. Zhang, L. Guo, S. Wei, Y. Y. He, H. Xia, Q. D. Chen, H. B. Sun, F. S. Xiao, *Nano Today* **2010**, *5*, 15.
[3] S. A. Baker, G. A. Baker, *Angew. Chem. Int. Ed.* **2010**, *49*, 6726.
[4] J. H. Shen, Y. H. Zhu, X. L. Yang, C. Z. Li, *Chem. Commun.* **2012**, *48*, 3686.
[5] S. J. Zhu, S. J. Tang, J. H. Zhang, B. Yang, *Chem. Commun.* **2012**, *48*, 4527.
[6] D. Y. Pan, J. C. Zhang, Z. Li, C. Wu, X. M. Yan, M. H. Wu, *Chem. Commun.* **201 0**, *46*, 3681.
[7] V. Gupta, N. Chaudhary, R. Srivastava, G. D. Sharma, R. Bhardwaj, S. Chand, *J. Am. Chem. Soc.* **201 1**, *133*, 9960.
[8] S. J. Zhuo, M. W. Shao, S. T. Lee, *ACS Nano* **2012**, *6*, 1059.
[9] D. Y. Pan, J. C. Zhang, Z. Li, M. H. Wu, *Adv. Mater.* **2010**, *22*, 734.
[10] X. Yan, X. Cui, L. S. Li, *J. Am. Chem. Soc.* **2010**, *132*, 5944.
[11] J. Peng, W. Gao, B. K. Gupta, Z. Liu, R. Romero-Aburto, L. H. Ge, L. Song, L. B. Alemany, X. B. Zhan, G. H. Gao, S. A. Vithayathil, B. A. Kaipparettu, A. A. Marti, T. Hayashi, J. J. Zhu, P. M. Ajayan, *Nano. Lett.* **2012**, *12*, 844.
[12] L. B. Tang, R. B. Ji, X. K. Cao, J. X. Lin, H. X. Jiang, X. M. Li, K. S. Teng, C. M. Luk, S. J. Zeng, J. H. Hao, S. P. Lau, *ACS Nano* **2012**, *6*, 5102.
[13] M. L. Mueller, X. Yan, B. Dragnea, L. S. Li, *Nano Lett.* **2011**, *11*, 56.
[14] M. L. Mueller, X. Yan, J. A. McGuire, L. S. Li, *Nano Lett.* **2010**, *10*, 2679.
[15] L. Wang, H. Y. Wang, B. R. Gao, L. Y. Pan, Y. Jiang, Q. D. Chen, W. Han, H. B. Sun, *IEEE J. Quantum Electron.* **2011**, *47*, 1177.
[16] B. R. Gao, H. Y. Wang, Y. W. Hao, L. M. Fu, H. H. Fang, Y. Jiang, L. Wang, Q. D. Chen, H. Xia, L. Y. Pan, Y. G. Ma, H. B. Sun, *J. Phys. Chem. B* **2010**, *114*, 128.
[17] L. Wang, H. Y. Wang, H. H. Fang, H. Wang, Z. Y. Yang, B. R. Gao, Q. D. Chen, W. Han, H. B. Sun, *Adv. Funct. Mater.* **2012**, *22*, 2783.
[18] S. J. Zhu, J. H. Zhang, X. Liu, B. Li, X. F. Wang, S. J. Tang, Q. N. Meng, Y. F. Li, C. Shi, R. Hu, B. Yang, *RSC Adv.* **2012**, *2*, 2717.
[19] J. Lu, P. S. E. Yeo, C. K. Gan, P. Wu, K. P. Loh, *Nat. Nanotechnol.* **2011**, *6*, 247.
[20] S. J. Zhu, J. H. Zhang, C. Y. Qiao, S. J. Tang, Y. F. Li, W. J. Yuan, B. Li, L. Tian, F. Liu, R. Hu, H. N. Gao, H. T. Wei, H. Zhang, H. C. Sun, B. Yang, *Chem. Commun.* **2011**, *47*, 6858.
[21] Y. Li, Y. Hu, Y. Zhao, G. Q. Shi, L. E. Deng, Y. B. Hou, L. T. Qu, *Adv. Mater.* **2011**, *23*, 776.
[22] Y. P. Sun, B. Zhou, Y. Lin, W. Wang, K. A. S. Femando, P. Pathak, M. J. Meziani, B. A. Harruff, X. Wang, H. F. Wang, P. J. G. Luo, H. Yang, M. E. Kose, B. L. Chen, L. M. Veca, S. Y. Xie, *J. Am. Chem. Soc.* **2006**, *128*, 7756.
[23] H. T. Li, X. D. He, Z. H. Kang, H. Huang, Y. Liu, J. L. Liu, S. Y. Lian, C. H. A. Tsang, X. B. Yang, S. T. Lee, *Angew. Chem. Int. Ed.* **2010**, *49*, 4430.

[24] C. O. Girit, J. C. Meyer, R. Erni, M. D. Rossell, C. Kisielowski, L. Yang, C. H. Park, M. F. Crommie, M. L. Cohen, S. G. Louie, A. Zettl, *Science* **2009**, *323*, 1705.
[25] G. Eda, Y. Y. Lin, C. Mattevi, H. Yamaguchi, H. A. Chen, I. S. Chen, C. W. Chen, M. Chhowalla, *Adv. Mater.* **2010**, *22*, 505.
[26] J. H. Shen, Y. H. Zhu, C. Chen, X. L. Yang, C. Z. Li, *Chem. Commun.* **2011**, *47*, 2580.
[27] X. Wang, L. Cao, S. T. Yang, F. S. Lu, M. J. Meziani, L. L. Tian, K. W. Sun, M. A. Bloodgood, Y. P. Sun, *Angew. Chem.* **2010**, *122*, 5438.
[28] S. Logunov, T. Green, S. Marguet, M. A. El-Sayed, *J. Phys. Chem. A* **1998**, *102*, 5652.
[29] K. Dohnalová, A. N. Poddubny, A. A. Prokofiev, W. DAM. de Boer, C. P. Umesh, J. MJ. Paulusse, H. Zuilhof, T. Gregorkiewicz, *Light: Science & Applications* **2013**, *2*, e47.
[30] D. Wang, L. Wang, X. Y. Dong, Z. Shi, J. Jin, *Carbon* **2012**, *50*, 2147.
[31] Q. S. Mei, K. Zhang, G. J. Guan, B. H. Liu, S. H. Wang, Z. P. Zhang, *Chem. Commun.* **2010**, *46*, 7319.
[32] Y. Li, Y. Zhao, H. H. Cheng, Y. He, G. Q. Shi, L. M. Dai, L. T. Qu, *J. Am. Chem. Soc.* **2012**, *134*, 15.
[33] L. L. Li, J. Ji, R. Fei, C. Z. Wang, Q. Lu, J. R. Zhang, L. P. Jiang, J. J. Zhu, *Adv. Funct. Mater.* **2012**, *22*, 2971.
[34] H. Tetsuka, R. Asahi, A. Nagoya, K. Okamoto, I. Tajima, R. Ohta, A. Okamoto, *Adv. Mater.* **2012**, *24*, 5333.
[35] Z. C. Yang, X. Li, J. Wang, *Carbon* **2011**, *49*, 5207.
[36] D. Y. Pan, L. Guo, J. C. Zhang, C. Xi, Q. Xue, H. Huang, J. H. Li, Z. W. Zhang, W. J. Yu, Z. W. Chen, Z. Li, M. H. Wu, *J. Mater. Chem.* **2012**, *22*, 3314.